Johann Radon Institute for
Computational and Applied Mathematics
Austrian Academy of Sciences (ÖAW)

Equilibrated Residual Error Estimator for Maxwell's Equations

D. Braess, J. Schöberl

RICAM-Report 2006-19

EQUILIBRATED RESIDUAL ERROR ESTIMATOR FOR MAXWELL'S EQUATIONS

DIETRICH BRAESS AND JOACHIM SCHÖBERL

Abstract. A posteriori error estimates without generic constants can be obtained by a comparison of the finite element solution with a feasible function for the dual problem. A cheap computation of such functions via equilibration is well-known for scalar equations of second order. We simplify and modify the equilibration such that it can be applied to Maxwell's equations and edge elements. The construction is more involved for edge elements since the equilibration has to be performed on subsets with different dimensions. For this reason, Raviart–Thomas elements are extended in the spirit of distributions.

1. Introduction

Recently, a posteriori error estimates without constants have attracted much interest; see Ainsworth and Oden [1], Neittaanmäki and Repin [16], Vejchodský [19], Luce and Wohlmuth [13] and also Ladeveze and Leguillon [12]. At first glance they look like estimators which use local Neumann problems as introduced by Bank and Weiser [5], but they are based on a comparison of primal and dual forms of the variational problems. Following Prager and Synge (1949) in the special case of the Poisson equation $-\Delta u = f$ in Ω, one compares a finite element approximation $u_h \in H^1(\Omega)$ and a function $\sigma \in H(\mathrm{div})$ which satisfies the equilibrium condition $\mathrm{div}\,\sigma + f = 0$. In principle, the latter can be obtained via mixed methods, but in practical computations a feasible function σ is constructed by an equilibration of ∇u_h.

The equilibration can be done by solving local problems; see [1, Chapter 6.4]. The solution of local problems by polynomials of sufficiently high order is avoided in [19] by the combination with a variant of the hypercircle method and in [13] by the introduction of a dual

1991 *Mathematics Subject Classification.* 65N30.

Key words and phrases. a posteriori error estimates, Maxwell equations.

The second author acknowledges support from the Austrian Science Foundation FWF within project grant Start Y-192, "hp-FEM: Fast Solvers and Adaptivity".

mesh. We will go a different way. A small portion of the error that results from the data oscillation is estimated in the classical manner. So the local problems become transparent, and a generalization to other types of elliptic problems is now natural (although not trivial). In the 2D case there is even a simple geometrical interpretation of the resulting equilibration procedure.

In the present paper we also establish a posteriori error estimators for Maxwell's equations with similar properties. There is an analogue to the result of Prager and Synge although we have to deal with different Sobolev spaces and edge elements. The equilibration in $H(\mathrm{curl})$, however, is more involved since the splitting of the residual currents into local divergence-free currents has to be done with more constraints. Moreover, the constraints refer to currents on geometrical objects with different dimensions.

To overcome these obstacles we proceed as we have shown for the Poisson equation. We extend the Raviart–Thomas elements and Nédélec elements to finite element spaces such that the differential operators curl and div act on distributions. We show that the differential operators and the extended spaces still form exact sequences. The sequences generalize the de Rham sequences and the discrete analoga that were frequently used in the last years for constructing and understanding new finite element spaces [2, 3, 11].

In Section 2 we write the equilibration procedure for the (scalar) Poisson equation in our setting in order to make the reader familiar with the new ideas. The resulting local problems will differ from those in [1, 13, 19]. The distributional Raviart–Thomas elements and the corresponding Nédélec elements are introduced in Section 3. Details are provided for the 2-dimensional case while the discussion of the 3-dimensional case is treated more briefly. Section 4 contains the application to a posteriori error estimators for Maxwell's equations.

The Sobolev spaces $H^1(\Omega)$, $H^1_0(\Omega)$, $H(\mathrm{div},\Omega)$ and $H(\mathrm{curl},\Omega)$ are defined as usual. The specification of the domain will be often suppressed when there is no danger of ambiguity.

2. Equilibrated Residual Error Estimates for Scalar Equations

In this section we consider the scalar equation

$$-\Delta u = f \tag{2.1}$$

on a polygonal domain Ω in 2-space or 3-space. Moreover, let $u = 0$ on a non-empty subset $\Gamma_D \subset \partial\Omega$ and $\partial u/\partial n = 0$ on $\Gamma_N := \partial\Omega\backslash\Gamma_D$. The application of a result by Prager and Synge for getting a posteriori

error estimates is well known although the presentation in the literature differs very much; see [17, 1, 12, 16, 13, 19]. We provide a review of the method and the essential ideas for the scalar equation (2.1) and establish simpler local problems in a framework which will be appropriate for Maxwell's equations in Section 4. For convenience, we restrict ourselves to the Poisson equation in this section. The generalization to equations with piecewise constant coefficients will be clear from the considerations in Section 4.

The finite element solutions are determined on a triangulation of Ω into triangles or tetrahedra, $\bar{\Omega} = \cup_T T$, and we decompose the L_2-functional

$$\langle f, v\rangle = \sum_T \int_T f v\,.$$

Moreover we introduce the integrals over elements

$$\widehat{f}^{\,T} = \int_T f\,. \tag{2.2}$$

Let

$$\mathcal{M}^k_{-1} := \{v \in L_2(\Omega);\ v|_T \in \mathcal{P}_k\}, \quad \mathcal{M}^k_0 := \mathcal{M}^k_{-1} \cap C^0(\Omega)$$

be the sets of polynomial Lagrange finite elements on the triangulation above, and let $u_h \in V_h := \mathcal{M}^1_0$ (with the essential boundary conditions incorporated) be the finite element solution for linear elements, i. e.

$$(\nabla u_h, \nabla v) = (f, v) \quad \text{for } v \in V_h\,. \tag{2.3}$$

The distribution

$$f_h := -\Delta u_h \tag{2.4}$$

is a functional on $H^1(\Omega)$ and evaluates to

$$\begin{aligned}\langle f_h, v\rangle &= (\nabla u_h, \nabla v) = \sum_T \left\{ -\int_T \Delta u_h\, v + \int_{\partial T} \frac{\partial u_h}{\partial n}\, v \right\} \\ &= \sum_F \int_F f_{h,F}\, v\,.\end{aligned}$$

Here F runs over the faces of the elements (and over the edges in the 2D-case, resp.), and

$$f_{h,F} = \left[\frac{\partial u_h}{\partial n}\right] := \frac{\partial u_{h,l}}{\partial n_l} + \frac{\partial u_{h,r}}{\partial n_r}\,.$$

Furthermore we introduce the corresponding integrals

$$\widehat{f}_h^{\,F} = \int_F f_{h,F}. \tag{2.5}$$

Since we treat here the d-dimensional case for $d = 2$ and $d = 3$ simultaneously, we use the letter F for the $d-1$-dimensional simplices. In general, contributions of tetrahedral/triangular elements, faces, edges and vertices are distinguished by the labels T, F, E, and V, respectively.

2.1. **The Theorem of Prager and Synge.**

Theorem 1. *(Theorem of Prager and Synge) Let $\sigma \in H(\mathrm{div})$, $\sigma \cdot n = 0$ on Γ_N while $v \in H^1(\Omega)$, $v = 0$ on Γ_D and assume that*

$$\operatorname{div} \sigma + f = 0. \tag{2.6}$$

Furthermore, let u be the solution of the Poisson equation (2.1). Then,

$$\|\nabla u - \nabla v\|^2 + \|\nabla u - \sigma\|^2 = \|\nabla v - \sigma\|^2. \tag{2.7}$$

Proof. For completeness, the short proof is included. By applying Green's formula we obtain

$$\int_\Omega \nabla(u - v)(\nabla u - \sigma) = -\int_\Omega (u - v)(\Delta u - \operatorname{div} \sigma) = 0,$$

because the boundary terms vanish. From this orthogonality relation we conclude that

$$\|\nabla v - \sigma\|^2 = \|\nabla(v - u)\|^2 + \|\nabla u - \sigma\|^2$$

which yields the desired relation (2.7). □

Now we are looking for a cheap construction of a function σ that satisfies (2.6).

First we assume that f is constant on each element. Then there is a function σ as required in the Raviart–Thomas space $\mathcal{R}T$:

$$\begin{aligned} \mathcal{R}T_{-1} &:= \{\tau \in [L_2(\Omega)]^d;\ \tau|_T = a_T + b_T x,\ a_T \in \mathbb{R}^d,\, b_T \in \mathbb{R}\ \forall T\}, \\ \mathcal{R}T &:= \mathcal{R}T_{-1} \cap H(\mathrm{div}). \end{aligned}$$

If we would solve the original equation (2.1) by the mixed method with the Raviart–Thomas element [8, p. 146], then we would yield the function $\sigma \in \mathcal{R}T$ with (2.6) for which

$$\|\nabla u_h - \sigma\|$$

is minimal. Indeed, it follows from (2.7) that this is equivalent to the minimization of $\|\nabla u - \sigma\|$, and here the minimum is known to be attained at the solution of the mixed method of Raviart–Thomas. This procedure, however, would be too expensive for computing a posteriori error estimates. One rather constructs an approximate solution from the given finite element solution u_h by a local procedure called *equilibration*. To be more precise, we emphasize that we perform the

construction for the difference $\sigma - \nabla u_h$ since there is a natural decomposition of this difference into functions with local support. – Both the functions σ and ∇u_h are contained in the *broken Raviart–Thomas space* $\mathcal{R}T_{-1}$ defined above.

2.2. **Equilibration.** In our context we write the residual as

$$f - f_h = -\operatorname{div} \sigma^\Delta. \tag{2.8}$$

Given a vertex V of the mesh, we assign to it the patch $\omega_V := \cup\{T,\, V \in \partial T\}$. The correction σ^Δ will be constructed from the solutions of local problems on patches:

$$\sigma^\Delta = \sum_V \sigma_{\omega_V}\,. \tag{2.9}$$

Here V runs over all vertices of the triangulation, and the support of σ_{ω_V} is contained in ω_V. – From (2.4) and (2.8) it follows that $\sigma := \nabla u_h + \sigma^\Delta \in H(\mathrm{div})$ satisfies $\operatorname{div}\sigma + f = 0$, and by Theorem 1 we have

$$\|\nabla u - \nabla u_h\|_{L_2} \le \|\sigma^\Delta\|_{L_2},$$

i. e. an upper bound with constant one. Note that we rather determine σ^Δ by local procedures (and not σ).

Now we turn to the construction of σ_{ω_V} in the 3D-case. We recall that f is assumed to be constant on each element. Let V be a node of the mesh and ψ_V be the linear nodal function with $\psi_V(V) = 1$ and $\psi_V(x) = 0$ for $x \in \Omega\backslash\omega_V$. From the characterization (2.3) of u_h as a finite element solution and by partial integration we obtain

$$\sum_{T\subset\omega_V} \int_T f\psi_V = \sum_{T\subset\omega_V} \int_T \nabla u_h \nabla\psi_V = \sum_{F\subset\omega_V} \int_F \Big[\frac{\partial u_h}{\partial n}\Big]\psi_V\,.$$

Since ψ_V is piecewise linear, we have for $d = 3$ the equations $\int_T \psi_V dx = \frac{1}{d+1}\int_T dx = \frac{1}{4}|T|$ and $\int_F \psi_V dx = \frac{1}{d}\int_F dx = \frac{1}{3}|F|$. Hence,

$$\frac{1}{4}\sum_{T\subset\omega_V} \int_T f = \frac{1}{3}\sum_{F\subset\omega_V} \int_F f_{h,F}$$

or with the notation (2.2) and (2.5)

$$\frac{1}{4}\sum_{T\subset\omega_V} \widehat{f}^{\,T} = \frac{1}{3}\sum_{F\subset\omega_V} \widehat{f}_h^{\,F}\,. \tag{2.10}$$

Now, we fix the local source term f_{ω_V} by defining its element and edge contributions:

$$\begin{aligned} \widehat{f}^T_{\omega_V} &:= \frac{1}{4}\widehat{f}^T, \\ \widehat{f}^F_{\omega_V} &:= -\frac{1}{3}\widehat{f}^F_h . \end{aligned} \tag{2.11}$$

Since each tetrahedron has 4 vertices and each face has 3 vertices, this is a decomposition of the global residual

$$f - f_h = \sum_V f_{\omega_V}.$$

It follows from (2.10) that the decomposition satisfies

$$\sum_T \widehat{f}^T_{\omega_V} + \sum_F \widehat{f}^F_{\omega_V} = 0 \tag{2.12}$$

for each V, i.e. $\langle f_{\omega_V}, 1\rangle = 0$.

Remark 2. *There are some modifications at the vertices on the boundary of Ω. If $\partial\omega_V \cap \partial\Omega \subset \Gamma_N$, there is no change apart from the geometry. If $V \in \Gamma_D$, then there is no test function associated with the vertex, and (2.12) does not hold for the vertex V. In this case, however, there is no boundary condition on $\partial\omega_V \cap \Gamma_D$ when we construct σ_{ω_V}. There is no problem. – Thus we will ignore adaptations at boundaries in the sequel.*

We obtain σ_{ω_V} in the broken RT space with support in ω_V and

$$\operatorname{div}\sigma_{\omega_V} + f_{\omega_V} = 0$$

by applying the following lemma to the patches ω_V. Specifically, each σ_{ω_V} is a solution of a local variational problem on a small patch. By summing over all patches a solution σ^Δ of (2.8) is constructed. Note that the normal components of the equilibrated functions are constant on the faces while the construction in [1, Chapter 6.4] generates functions with piecewise linear normal components.

Lemma 3. *Let $\omega = \cup_T T \subset \mathbb{R}^d$, $d = 2$ or 3, be simply connected, and let $\cup_F F = \cup_T \partial T \backslash \partial\omega$ be a decomposition of the interelement boundaries. If the distribution g,*

$$\langle g, v\rangle := \sum_T \int_T g_T v + \sum_F \int_F g_F v \tag{2.13}$$

with piecewise constant functions g_T, g_F satisfies $\langle g, 1\rangle = 0$, then there exists $\sigma \in \mathcal{R}T_{-1}$ such that

$$\begin{aligned} \sigma \cdot n &= 0 \quad \text{on } \partial\omega, \\ \operatorname{div}\sigma &= g_T \quad \text{in } T, \\ [\sigma \cdot n] &= g_F \quad \text{on } F. \end{aligned} \tag{2.14}$$

Moreover, there exists a constant c depending only on the shape parameter of the mesh such that

$$\|\sigma\|_0^2 \le c\Big(\sum_T h_T^2 \|g_T\|_{L_2(T)}^2 + \sum_F h_F \|g_F\|_{L_2(F)}^2\Big).$$

Proof. First we reduce the given equations to a problem without face terms. We choose $\sigma^1 \in \mathcal{R}T_{-1}$ by setting

$$\sigma^1 \cdot n = -\frac{1}{2}\, g_F \quad \text{at internal interfaces}$$

and $\sigma^1 \cdot n = 0$ on $\partial\omega$. Thus, the face contributions of $\operatorname{div}\sigma^1$ coincide with the face contributions of g, and the difference is the regular function

$$g - \operatorname{div}\sigma^1 \in \mathcal{M}^0_{-1} \quad \text{and} \quad \big\langle g - \operatorname{div}\sigma^1, 1\big\rangle = 0.$$

From Remark 2.1 in [3] we know that the sequence

$$\mathcal{R}T_{0,0} \xrightarrow{\operatorname{div}} \mathcal{M}^0_{-1} \xrightarrow{\int 1} \mathbb{R} \tag{2.15}$$

is exact, where $\mathcal{R}T_{0,0} := \{\tau \in \mathcal{R}T_{-1},\ \tau \cdot n = 0 \text{ on } \partial\omega\}$ and the second mapping is defined by $\int 1 : g \mapsto \langle g, 1\rangle$. Thus there exists $\sigma^0 \in \mathcal{R}T$ such that

$$\begin{aligned} \operatorname{div}\sigma^0 &= g - \operatorname{div}\sigma^1 \quad \text{in } \omega, \\ \sigma^0 \cdot n &= 0 \quad \text{on } \partial\omega. \end{aligned}$$

Setting $\sigma := \sigma^0 + \sigma^1$ we obtain a solution of (2.14). The stability estimate will be proven in Section 3.4 for more general cases. (It is also not difficult to obtain it in the 2D case from Algorithm 4.) □

The first result of the lemma can be understood as an extension of (2.15) being an exact sequence. Let

$$\begin{aligned} \mathcal{R}T_{-1,0} &:= \{\tau \in \mathcal{R}T_{-1},\ \tau \cdot n = 0 \text{ on } \partial\omega\}, \\ \mathcal{M}^0_{-2} &:= \{g \in H^1(\omega))',\ \langle g, v\rangle := \sum_T \int_T g_T v + \sum_F \int_F g_F v, \\ &\qquad g_T, g_E \in \mathbb{R}\}. \end{aligned}$$

Then the sequence

$$\mathcal{R}T_{-1,0} \xrightarrow{\operatorname{div}} \mathcal{M}^0_{-2} \xrightarrow{\int 1} \mathbb{R} \tag{2.16}$$

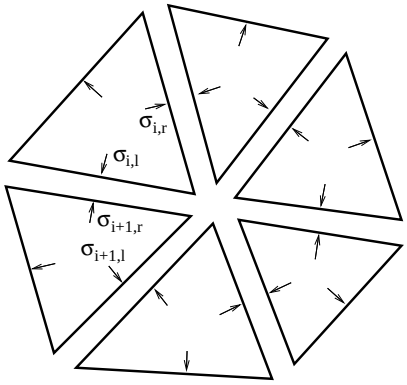

FIGURE 1. Fluxes in a patch around a vertex V. $\sigma_{i,r}$ and $\sigma_{i,l}$ are the normal components of the fluxes that leave the triangle T_i on the right and left side, respectively. The triangles are enumerated counterclockwise and $E_i = T_i \cap T_{i+1}$ (with indices modulo the number of triangles).

is exact.

2.3. **Equilibration in 2D.** In the 2-dimensional case the solution of the equation $\operatorname{div} \sigma_{\omega_V} + f_{\omega_V} = 0$ can be easily solved by geometrical arguments. They also show that our procedure differs from that one presented by Ainsworth and Oden [1].

We obtain (in the 2D case)

$$\frac{1}{3} \sum_{T \subset \omega_V} \widehat{f}^{\,T} = \frac{1}{2} \sum_{E \subset \omega_V} \widehat{f}_h^{\,E} \,. \tag{2.17}$$

instead of (2.10). This is consistent with the fact that each triangle T has 3 vertices and each edge lies between 2 vertices. A decomposition with $\widehat{f}_{\omega_V}^{\,T} := \frac{1}{3}\widehat{f}^{\,T}$ and $\widehat{f}_{\omega_V}^{\,E} := -\frac{1}{2}\widehat{f}_h^{\,E}$ implies that (2.12) holds again.

The desired function σ_{ω_V} will be given in terms of $\sigma_{\omega_V} \cdot n$ on the edges in ω_V; see Figure 1 for the notation. By definition we have $\sigma_{\omega_V} \cdot n = 0$ on the edges on the boundary of ω_V. We have to determine $\sigma_{\omega_V} \cdot n$ only on the edges which are adjacent to V. Since σ_{ω_V} is a broken RT function, the values on both sides of an edge have to be specified. Specifically, we determine the integrals

$$\widehat{\sigma_{i,l}} := \int_{E_l} \sigma_{i,l} \cdot n \,, \qquad \widehat{\sigma_{i,r}} := \int_{E_{l-1}} \sigma_{i,r} \cdot n \,.$$

By Gauss' theorem the (constant) divergence in a triangle is given by the flux over the two edges that are adjacent to V. Therefore, we

have for $\sigma = \sigma_{\omega_V}$ with the notation in Figure 1:

$$\widehat{\sigma_{i,r}} + \widehat{\sigma_{i,l}} = \int_{\partial T_i} \sigma_{\omega_V} \cdot n = \int_{T_i} \operatorname{div} \sigma_{\omega_V} = -\widehat{f_{\omega_V}}^{T_i}. \tag{2.18}$$

Moreover the jump on each edge is fixed such that

$$\widehat{\sigma_{i,l}} + \widehat{\sigma_{i+1,r}} = \int_E [\sigma_{\omega_V} \cdot n] = \widehat{f_{\omega_V}}^{E_i}. \tag{2.19}$$

From (2.17) it follows that these conditions are consistent, and they can be satisfied when we transverse around the node V. The following algorithm produces a σ_{ω_V} such that (2.18) and (2.19) are satisfied.

Algorithm 4 (for the construction of σ_{ω_V})**.**
set $\sigma_{1,r} = 0$.
for $i = 1, 2, \ldots$ *until an entire circuit around* V *is completed*

$$\begin{array}{l}\{\\ \widehat{\sigma_{i,l}} = -\widehat{f_{\omega_V}}^{T_i} - \widehat{\sigma_{i,r}},\\ \widehat{\sigma_{i+1,r}} = +\widehat{f_{\omega_V}}^{E_i} - \widehat{\sigma_{i,l}}\\ \}\end{array}$$

Let c *be the mean value of all the differences* $(\widehat{\sigma_{i,l}} - \widehat{\sigma_{i,r}})$. *Add* $c/2$ *to each* $\widehat{\sigma_{i,r}}$ *and subtract it from each* $\widehat{\sigma_{i,l}}$. □

The last correction implies that we minimize $\|\widehat{\sigma}\|_{\mathbb{R}^n}$.

2.4. **Data Oscillation.** Eventually, we want to abandon the assumption that f is piecewise constant. Let $\bar{f}$ be the L_2 projection of f onto piecewise constant functions. The preceding investigation applies to the error if the right-hand side of (2.1) is replaced by $\bar{f}$. In order to guarantee (2.12) we have to set $\widehat{f}_{\omega_V}^T := \int_T f\psi_V$ and cannot use the simple factor 1/4 as in (2.11). This is no drawback since $\sum_V \int_T f\psi_V = |T|\hat{f}_T$ and the integrals $\int_T f\psi_V$ have been computed with the assembling of the finite element equations.

Now the difference between the solution for f and $\bar{f}$ can be bounded by

$$ch\|f - \bar{f}\|. \tag{2.20}$$

This effect of the *data oscillation* is well-known [8, p. 171]. We emphasize that the constant c depends on the shape of the elements, but it does not depend on the domain Ω. Since (2.20) is a term of higher order, we admit a generic constant here.

2.5. **Efficiency.** By construction the error estimate

$$\|\nabla(u-u_h)\| \le \|\sigma^\Delta\| + ch\|f-\bar f\|$$

is reliable. The efficiency has been less discussed in the literature. By Lemma 3 $\|\sigma^\Delta\|$ can be bounded by the terms $h_T\|f_T\|$ and $h_f^{1/2}\|f_{h,F}\|$, i.e. by the ingredients of the well-known residual error estimator. Thus $\|\sigma^\Delta\|$ is bounded by a multiple of that estimator. Since the residual error estimator is efficient, the same holds for the estimates determined by equilibration.

The results of this section are summarized for the Poisson equation in d-space as follows.

Theorem 5. *For each node V there exists a broken RT-function σ_{ω_V} with support in ω_V and*

$$\begin{aligned} \operatorname{div}\sigma_{\omega_V} &= \tfrac{1}{|T|}\textstyle\int_T f\psi_V && \text{in } T\subset\omega_V,\\ [\sigma_{\omega_V}\cdot n] &= -\tfrac{1}{d}[\nabla u_h\cdot n] && \text{on } F\subset\omega_V,\\ \sigma_{\omega_V}\cdot n &= 0 && \text{on } \partial\omega_V. \end{aligned}$$

Choose σ_{ω_V} with (quasi-) minimal L_2-norm, and let $\sigma^\Delta := \sum_V \sigma_{\omega_V}$. Then we have the a posteriori error estimate

$$c_0\|\sigma^\Delta\| - ch\|f-\bar f\| \le \|\nabla(u-u_h)\| \le \|\sigma^\Delta\| + ch\|f-\bar f\|. \quad (2.21)$$

3. Distributional Finite Element de Rham Sequences

In the treatment of the scalar equation we already encountered distributional finite elements. In this section, we introduce and study exact sequences of finite elements which contain more distributional terms and are suitable for Maxwell's equations.

We start with the two dimensional case and continue with three dimensional finite elements.

Let Ω be a simply connected domain in $\mathbb{R}^2$. In 2D, we write curl for the differential operator $(\frac{\partial}{\partial y}, -\frac{\partial}{\partial x})$. Then, the de Rham sequence

$$\mathbb{R} \longrightarrow H^1 \xrightarrow{\text{curl}} H(\text{div}) \xrightarrow{\text{div}} L_2 \longrightarrow 0 \quad (3.1)$$

is an exact sequence [2]. This means that

- the operator curl has a trivial kernel in $H^1/\mathbb{R}$;
- the kernel $\{\sigma \in H(\text{div}) : \text{div}\,\sigma = 0\}$ of the operator div is exactly the range of the operator curl;
- the range of the operator div is exactly L_2.

An analogous property holds for the spaces with zero boundary conditions H_0^1 and $H_0(\mathrm{div}) := \{\sigma \in H(\mathrm{div}) : \sigma \cdot n = 0 \text{ on } \partial\Omega\}$:

$$0 \longrightarrow H_0^1 \xrightarrow{\mathrm{curl}} H_0(\mathrm{div}) \xrightarrow{\mathrm{div}} L_2 \xrightarrow{\int 1} \mathbb{R} \longrightarrow 0. \tag{3.2}$$

As usual, the space $L_{2,0} := \{f \in L_2 : \int_\Omega f = 0\}$ of functions with zero mean values is identified with $L_2/\mathbb{R}$. We focus on sequences without boundary conditions, i.e., on sequences of type (3.1) in the following introductory discussion although we will deal later also with generalizations of (3.2).

Note that we find the right-hand part of the last exact sequence on the discrete level in (2.15) and (2.16).

3.1. **First Distributional Triangular Elements.** The exact sequence property is inherited on the discrete level when we choose piecewise linear and continuous Lagrangian elements $\mathcal{M}_0^1$ for modeling H^1, the Raviart–Thomas elements $\mathcal{R}T$ for $H(\mathrm{div})$, and piecewise constant, non-continuous elements $\mathcal{M}_{-1}^0$ for L_2, [7, p. 175]:

$$\mathbb{R} \longrightarrow \mathcal{M}_0^1 \xrightarrow{\mathrm{curl}} \mathcal{R}T \xrightarrow{\mathrm{div}} \mathcal{M}_{-1}^0 \longrightarrow 0. \tag{3.3}$$

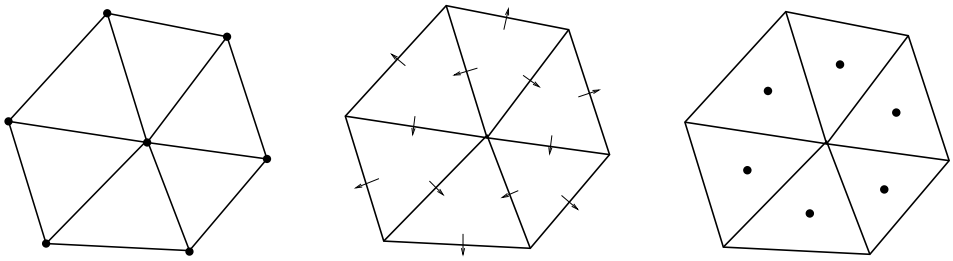

FIGURE 2. Classical finite element spaces in the sequence (3.3).

Let $u \in \mathcal{M}_0^1$, $\sigma \in \mathcal{R}T$, and $f \in \mathcal{M}_{-1}^0$. Their natural degrees of freedom are nodal values $\widehat{u}^{\,V} := u(V)$, edge integrals of the normal components $\widehat{\sigma}^{\,E} := \int_E \sigma \cdot n$, and element integrals $\widehat{f}^{\,T} := \int_T f$, respectively. Note that an orientation is associated to each edge for defining the normal components of RT functions.

The representation of the differential operators with respect to these degrees of freedom depends only on the element topology and is independent of the shape of the elements. In terms of degrees of freedom we find

$$\sigma = \operatorname{curl} u \quad \text{as} \quad \widehat{\sigma}^{\,E} = \widehat{u}^{\,V_{E,1}} - \widehat{u}^{\,V_{E,2}},$$

where $V_{E,1}$ and $V_{E,2}$ are the two vertices of the edge E, ordered consistently with the previously defined normal vector. Similarly, the expression

$$f = \operatorname{div} \sigma \quad \text{reads as} \quad \widehat{f}^{\,T} = \sum_{E \subset T} \pm \widehat{\sigma}^{\,E},$$

where the sign depends on the orientation of the normal vector. Specifically, the sign is positive for normal vectors pointing to the outside of the triangle.

An element f in $\mathcal{M}^0_{-1}$ generates the regular distribution

$$\langle f, v \rangle = \sum_T \int_T f_T v.$$

For our purposes we introduce the space $\mathcal{M}^0_{-3}$ of distributions involving element, edge, and vertex terms:

$$\langle f, v \rangle = \sum_T \int_T f_T v + \sum_E \int_E f_E v + \sum_V f_V v(V). \tag{3.4}$$

The functions f_T and f_E are constant on each triangle and edge, respectively. The subspace of distributions of the form (3.4) with vanishing vertex terms is denoted as $\mathcal{M}^0_{-2}$.

First, we restrict ourselves to those distributions with element and vertex terms, i.e. with $f_V = 0$ for all V; see also (2.13). In this context we recall the extension of the Raviart–Thomas space to the broken Raviart–Thomas space, and obtain the *first distributional de Rham sequence*

$$\mathbb{R} \longrightarrow \mathcal{M}^1_0 \xrightarrow{\text{curl}} \mathcal{R}T_{-1} \xrightarrow{\text{div}} \mathcal{M}^0_{-2} \longrightarrow 0. \tag{3.5}$$

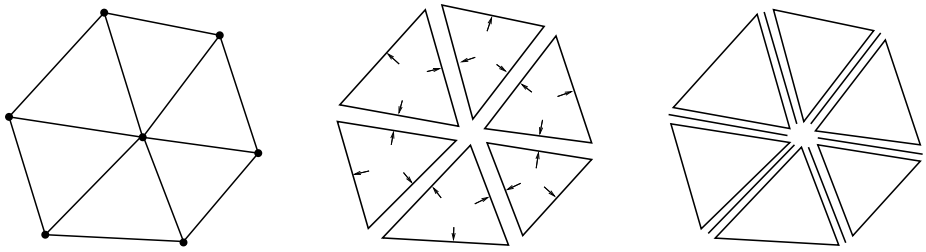

FIGURE 3. Distributional finite element spaces in the sequence (3.5). The middle lines of the edges represent the edge terms in (3.4).

The sequence (3.5) is well defined. This is clear for the curl operator. To verify it for the divergence, let $\sigma \in \mathcal{R}T_{-1}$, and define $f = \operatorname{div} \sigma$ in

distributional sense by

$$\langle f, v\rangle := -\langle \sigma, \nabla v\rangle \quad \text{for } v \in C_0^\infty.$$

Integration by parts leads to

$$\begin{aligned}\langle f, v\rangle &= -\sum_T \int_T \sigma \cdot \nabla v \\ &= \sum_T \int_T \operatorname{div}_T \sigma\, v - \int_{\partial T} \sigma \cdot n\, v \\ &= \sum_T \int_T \operatorname{div}_T \sigma\, v - \sum_E \int_E \sum_{T:E\subset T} \sigma_T \cdot n_E\, v.\end{aligned}$$

Here the normal vectors are defined element by element and as usual in the outgoing direction; cf. Figure 3. Thus the image $\operatorname{div}\sigma$ belongs to $\mathcal{M}^0_{-2}$, and the relation $f = \operatorname{div}\sigma$ evaluates to two relations

$$f_T = \operatorname{div}_T \sigma_T \qquad \text{and} \qquad f_E = -\sum_{T:E\subset T} \sigma_T \cdot n_E\,. \tag{3.6}$$

Since $\sigma \in \mathcal{R}T_{-1}$ is determined by the fluxes on each side of the edges, we have in terms of degrees of freedom

$$\widehat{f}^{\,T} = \sum_{E\subset T} \widehat{\sigma_T}^{\,E} \qquad \text{and} \qquad \widehat{f}^{\,E} = -\sum_{T:E\subset T} \widehat{\sigma_T}^{\,E}.$$

Theorem 6. *The sequence (3.5) is exact.*

Proof. We recall that the classical sequence (3.3) is exact [2, 7, 9, 11, 14].

Due to (3.6) the properties $\sigma \in \mathcal{R}T_{-1}$ and $\operatorname{div}\sigma = 0$ imply that $\sigma \in \mathcal{R}T$. Hence, the divergence is defined as usual in $H(\operatorname{div})$ and vanishes. Now the exactness of (3.3) guarantees that Raviart–Thomas elements with vanishing divergence are curls of functions in $\mathcal{M}^1_0$.

The surjectivity of the divergence onto $\mathcal{M}^0_{-2}$ is also obtained from the exactness (3.3) by similar arguments as for the reduction in the proof of Lemma 3 (cf. also the reduction in the proof of the next theorem). □

3.2. **Second Distributional Triangular Elements.** For the treatment of Maxwell's equations, we need another extension of the sequence. Distributional elements on edges are added to the finite elements that model $H(\operatorname{div})$. Moreover, the full set $\mathcal{M}^0_{-3}$ of distributions of the form (3.4) enter into the theory.

The associated sequence will be called the *second distributional de Rham sequence*:

$$\mathbb{R} \longrightarrow \mathcal{M}^1_{-1} \xrightarrow{\text{curl}} \mathcal{R}T_{-2} \xrightarrow{\text{div}} \mathcal{M}^0_{-3} \longrightarrow 0. \tag{3.7}$$

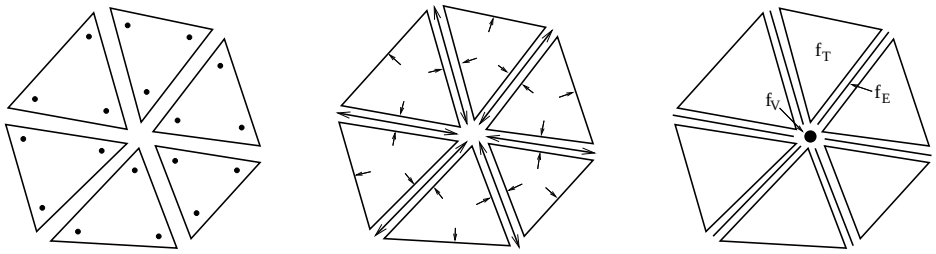

FIGURE 4. Distributional finite element spaces in the sequence (3.7). The arrows along the edges represent the edge and the vertex terms in (3.8).

The space $\mathcal{M}^1_{-1}$ consists of piecewise linear and non-continuous finite elements. The degrees of freedom are the values $\widehat{u_T}^V$ at the three vertices of each triangle; see Figure 4.

The corresponding Raviart–Thomas distributions are of the form

$$\langle \sigma, v \rangle = \sum_T \int_T \sigma_T \cdot v + \sum_E \int_E \sigma_E \cdot v,$$

where $\sigma_T = \vec{a} + b\vec{x}$, and $\sigma_E = (a + bx)\vec{\tau}_E$ are 1D Raviart–Thomas elements mapped to the edge where $\vec{\tau}_E$ is a tangential vector. The degrees of freedom are

$$\widehat{\sigma_T}^E = \int_E \sigma_T \cdot n_E \qquad \text{and} \qquad \widehat{\sigma_E}^V = \sigma_E(V) \cdot n_V. \tag{3.8}$$

Here n_V is the vector pointing outwards at the vertex V of an edge E.

The representation of the operation $f = \operatorname{div} \sigma$ in terms of the degrees of freedom is

$$\begin{aligned} \widehat{f}^T &= \sum_{E \subset T} \widehat{\sigma_T}^E, \\ \widehat{f}^E &= \sum_{V \in E} \widehat{\sigma_E}^V - \sum_{T : E \subset T} \widehat{\sigma_T}^E, \\ \widehat{f}^V &= -\sum_{E : V \in E} \widehat{\sigma_E}^V. \end{aligned} \tag{3.9}$$

Remark 7. *In contrast to the previous case,* $\operatorname{div} \sigma = 0$ *is now possible for elements* σ *which are not in the classical Raviart–Thomas space* $\mathcal{R}T$*. The distributional parts of* $\operatorname{div} \sigma$ *may add to zero in (3.9). Nevertheless, there is a geometrical understanding. We may blow up the*

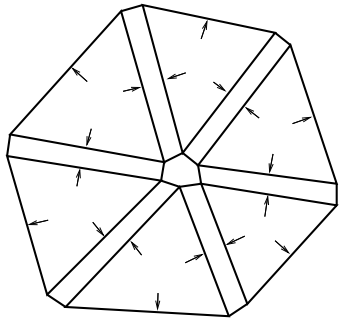

FIGURE 5. Slim rectangles in the sense of Remark 7.

edges to slim rectangles*; see Figure 5. If the divergence vanishes in the distributional sense, the total flow over the boundary of a slim rectangle (and not only over the boundary of the triangles) is zero.*

The imagination with the slim rectangles has another advantage. The (classical) Raviart–Thomas elements in 2-space are given by the fluxes on the edges. Now all the degrees of freedom of the distributional Raviart–Thomas elements are fluxes on edges, i.e., they live on 1-dimensional objects. The terms on the right-hand side of (3.9) are fluxes over boundaries of triangles, slim rectangles, or the central area in Figure 5.

The differential operation $\sigma = \operatorname{curl} u$ reads as

$$\begin{aligned} \widehat{\sigma_T}^E &= \widehat{u_T}^{V_{E,1}} - \widehat{u_T}^{V_{E,2}} \\ \widehat{\sigma_E}^V &= \widehat{u_{T_1}}^V - \widehat{u_{T_2}}^V, \end{aligned} \tag{3.10}$$

where T_1 is the left and T_2 is the right triangle when looking into the direction of n_v.

Theorem 8. *The second distributional de Rham sequence is exact.*

Proof. We start with proving that the operator div is a mapping onto $\mathcal{M}^0_{-3}$. Given $f \in \mathcal{M}^0_{-3}$, we first choose σ^2 such that the vertex terms of $\operatorname{div}\sigma^2$ coincide with the vertex terms of f. To this end we set

$$\widehat{\sigma^2_E}^V = -\frac{1}{N_V}\widehat{f}^V,$$

where N_V is the number of edges sharing the vertex V. From $(3.9)_3$ we know that

$$f - \operatorname{div}\sigma^2 \in \mathcal{M}^1_{-2}.$$

By the first distributional exact sequence, there exists $\sigma^1 \in \mathcal{R}T_{-1}$ such that $\operatorname{div}\sigma^1 = f - \operatorname{div}\sigma^2$. Hence,

$$\operatorname{div}(\sigma^1 + \sigma^2) = f.$$

This proves that the divergence operator is surjective and the exactness of the second operator.

Next, consider $\sigma \in \mathcal{R}T_{-2}$ with $\operatorname{div}\sigma = 0$. We construct a function $u^2 \in \mathcal{M}^1_{-1}$ such that the edge terms of $\operatorname{curl} u^2$ coincide with the edge terms of the given σ. This is done by a local construction for each vertex. Given a vertex V, we conclude from the vertex part of $\operatorname{div}\sigma$ that

$$\sum_{E:V\in E} \widehat{\sigma_E}^V = 0.$$

Now, enumerate the triangles sharing the vertex V from 1 to N_V. Enumerate the edges such that E_i is between triangle T_i and $T_{i+1 \bmod N_V}$. We set

$$u^2_{T_1}(V) = 0 \qquad \text{and} \qquad u^2_{T_{i+1}}(V) = u^2_{T_i}(V) + \widehat{\sigma_{E_i}}^V.$$

Since the vertex currents sum up to 0, it follows that

$$u^2_{T_1}(V) = u^2_{T_{N_V}}(V) + \widehat{\sigma_{E_{N_V}}}^V.$$

By construction, the edge terms of $\operatorname{curl} u^2$ coincide with the edge terms of σ. Thus, the difference satisfies

$$\sigma - \operatorname{curl} u^2 \in \mathcal{R}T_{-1} \qquad \text{and} \qquad \operatorname{div}(\sigma - \operatorname{curl} u^2) = 0.$$

We know from Theorem 6 that there exists $u^1 \in \mathcal{M}^1_0$ such that $\operatorname{curl} u^1 = \sigma - \operatorname{curl} u^2$, and $u = u^1 + u^2$ is the desired function in $\mathcal{M}^1_{-1}$. □

3.3. **Distributional Tetrahedral Elements.** The three-dimensional de Rham sequence contains an additional space. In the case of zero boundary conditions it reads

$$0 \longrightarrow H^1_0 \xrightarrow{\text{grad}} H_0(\text{curl}) \xrightarrow{\text{curl}} H_0(\text{div}) \xrightarrow{\text{div}} L_2 \xrightarrow{\int 1} \mathbb{R} \longrightarrow 0. \quad (3.11)$$

The canonical lowest order finite elements inherit the exact sequence property

$$0 \longrightarrow \mathcal{M}^1_0 \xrightarrow{\text{grad}} \mathcal{N}d \xrightarrow{\text{curl}} \mathcal{R}T \xrightarrow{\text{div}} \mathcal{M}^0_{-1} \xrightarrow{\int 1} \mathbb{R} \longrightarrow 0, \quad (3.12)$$

see [14]. Here, $\mathcal{N}d$ consists of the lowest order Nédélec elements.

We define the space $\mathcal{M}^0_{-4}$ of scalar distributions of the form

$$\langle f, v\rangle = \sum_T \int_T f_T v + \sum_F \int_F f_F v + \sum_E \int_E f_E v + \sum_V f_V v(V), \quad (3.13)$$

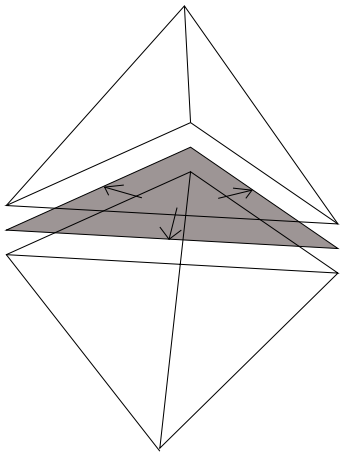

FIGURE 6. Raviart Thomas face distribution

where f_T, f_F, and f_E are piecewise constant functions on tetrahedra, faces, and edges, respectively. The f_V are real numbers. The subspaces $\mathcal{M}^0_{-1} \subset \mathcal{M}^0_{-2} \subset \mathcal{M}^0_{-3}$ of lower distributional orders are defined to contain

only element terms,

element and face terms, and

element, face, and edge terms, respectively.

Moreover, we define the space $\mathcal{RT}_{-3}$ of $H(\mathrm{div})$ distributions of the form

$$\langle \sigma, v \rangle = \sum_T \int_T \sigma_T \cdot v + \sum_F \int_F \sigma_F \cdot v + \sum_E \int_E \sigma_E \cdot v, \tag{3.14}$$

where σ_T, σ_F, and σ_E are in the Raviart–Thomas element space on tetrahedra T, triangular faces F in 3D space, and edges E in 3D. The degrees of freedom are the normal fluxes through the boundary. Specifically, we take the normal flux $\widehat{\sigma_T}^F$ of σ_T through the face $F \subset \partial T$, the normal flux $\widehat{\sigma_F}^E$ of σ_F through the edge $E \subset \partial F$, and the flux $\widehat{\sigma_E}^V$ of σ_E into the vertex V of E. The degrees $\widehat{\sigma_F}^E$ of a face flux are depicted in Figure 6.

Only element and face distributions are required for modeling the space $H(\mathrm{curl})$,

$$\langle H, v \rangle = \sum_T \int_T H_T \cdot v + \sum_F \int_F H_F \cdot v. \tag{3.15}$$

These distributions generate the space $\mathcal{N}d_{-2}$, and $\mathcal{N}d_{-1}$ is the sub-space with vanishing face terms. The finite element functions are spanned in each tetrahedron and triangle by Nédélec shape functions. Their degrees of freedom are the tangential components along the tetrahedral

and triangular edges. Note that there are jumps of the tangential components of a distributional Nédélec function between the tetrahedra, and individual values of the components are given on common edges.

Now we are ready to formulate three sequences for distributional finite element spaces in $\mathbb{R}^3$. They differ by the order of the distributions. We focus on the spaces with boundary conditions (but the sequences for the versions without boundary conditions are also exact):

$$0 \longrightarrow \mathcal{M}^1_0 \xrightarrow{\text{grad}} \mathcal{N}d_0 \xrightarrow{\text{curl}} \mathcal{R}T_{-1} \xrightarrow{\text{div}} \mathcal{M}^0_{-2} \xrightarrow{\int 1} \mathbb{R} \longrightarrow 0, \quad (3.16)$$

$$0 \longrightarrow \mathcal{M}^1_0 \xrightarrow{\text{grad}} \mathcal{N}d_{-1} \xrightarrow{\text{curl}} \mathcal{R}T_{-2} \xrightarrow{\text{div}} \mathcal{M}^0_{-3} \xrightarrow{\int 1} \mathbb{R} \longrightarrow 0, \quad (3.17)$$

$$0 \longrightarrow \mathcal{M}^1_{-1} \xrightarrow{\text{grad}} \mathcal{N}d_{-2} \xrightarrow{\text{curl}} \mathcal{R}T_{-3} \xrightarrow{\text{div}} \mathcal{M}^0_{-4} \xrightarrow{\int 1} \mathbb{R} \longrightarrow 0. \quad (3.18)$$

The first sequence (3.16) was already used for the construction of the equilibrated fluxes for the scalar equation in the previous section. The second sequence (3.17) will be used to construct the equilibrated magnetic fields for Maxwell's equations. The third one is formulated only for completeness.

Lemma 9. *The sequences (3.16), (3.17), and (3.18) are exact.*

Proof. We start with the first sequence. The exactness of $\mathcal{R}T_{-1} \xrightarrow{\text{div}} \mathcal{M}^0_{-2} \xrightarrow{\int 1} \mathbb{R}$ was already proven in Lemma 3. Since $\operatorname{div}\sigma = 0$ for $\sigma \in \mathcal{R}T_{-1}$ implies that $\sigma \in \mathcal{R}T$, the exactness of the rest of the sequence follows from the exactness of the standard finite element sequence.

We continue with the sequence (3.17). Given $f \in \mathcal{M}^0_{-3}$ that contains element, face, and edge terms, we construct a $\sigma \in \mathcal{R}T_{-2}$ such that $\operatorname{div}\sigma = f$. We define the edge degrees of freedom for an auxiliary σ^1 by

$$\widehat{\sigma^1{}_F}^E := \frac{1}{N_E}\widehat{f}^E,$$

where N_E is the number of faces sharing the edge E. Thus, the edge terms of $\operatorname{div}\sigma^1$ are equal to the edge terms of f, and thus $f - \operatorname{div}\sigma \in \mathcal{M}^0_{-2}$. The first distributional sequence yields the existence of a $\sigma^2 \in \mathcal{R}T_{-1}$ satisfying $\operatorname{div}\sigma^2 = f - \operatorname{div}\sigma^1$, and we have

$$\operatorname{div}(\sigma^1 + \sigma^2) = f.$$

We turn to the middle part of (3.17). Given $\sigma \in \mathcal{R}T_{-2}$ with $\operatorname{div}\sigma = 0$, we construct a function $H \in \mathcal{N}d_{-1}$ such that $\operatorname{curl} H = \sigma$. From the edge part of the divergence it follows that $\sum_{F:E\subset F} \widehat{\sigma_F}^E = 0$. We fix an edge E, and enumerate the tetrahedra and faces around the edges

such that face F_i is between T_i and T_{i+1}. Also here, element indices are taken modulo N_E. We define an H^1 by

$$\widehat{H^1_{T_1}}^E := 0 \qquad \text{and} \qquad \widehat{H^1_{T_{i+1}}}^E := \widehat{H^1_{T_i}}^E + \widehat{\sigma_{F_i}}^E.$$

Since $\operatorname{div}\sigma = 0$, we end up with $\widehat{H^1_{T_{N+1}}}^E = 0$ after a complete cycle. The residual $\sigma - \operatorname{curl} H^1$ is divergence free, and it is contained in $\mathcal{R}T_{-1}$. We apply the first distributional sequence to ensure the existence of an $H^2 \in \mathcal{N}d_0$ such that

$$\operatorname{curl}(H^1 + H^2) = \sigma.$$

To complete the second part, we pick an $H \in \mathcal{N}d_{-1}$ such that $\operatorname{curl} H = 0$. By definition $H \in L_2$ holds as well as $\operatorname{curl} H = 0 \in L_2$, thus $H \in H(\operatorname{curl})$. This implies that the tangential components of H are continuous, i.e., $H \in \mathcal{N}d$. By the exactness of the standard sequence, there exists a $\varphi \in \mathcal{M}^1_0$ such that $\operatorname{grad}\varphi = H$.

We skip the proof of the third sequence since it follows the same lines and it was added only for completeness. □

3.4. **Stability of Inverses.** For $f \in \mathcal{M}^0_{-4}$, $\sigma \in \mathcal{R}T_{-3}$, $H \in \mathcal{N}d_{-2}$, and $u \in \mathcal{M}^1_{-1}$ we define the mesh-dependent norms

$$\begin{aligned}
\|f\|^2_{0,h} &:= \sum_T \|f_T\|^2_{L_2(T)} + \sum_F h_F \|f_F\|^2_{L_2(F)} + \sum_E h_E^2 \|f_E\|^2_{L_2(E)} \\
&\quad + \sum_V h_V^3 |f_V|^2, \\
\|\sigma\|^2_{0,h} &:= \sum_T \|\sigma_T\|^2_{L_2(T)} + \sum_F h_F \|\sigma_F\|^2_{L_2(F)} + \sum_E h_E^2 \|\sigma_E\|^2_{L_2(E)}\,, \\
\|H\|^2_{0,h} &:= \sum_T \|H_T\|^2_{L_2(T)} + \sum_F h_F \|H_F\|^2_{L_2(F)}\,, \\
\|u\|^2_{0,h} &:= \sum_T \|u_T\|^2_{L_2(T)}\,.
\end{aligned}$$

Lemma 10. *The right inverses of the differential operators constructed above satisfy the norm estimates*

$$\begin{aligned}
\|\sigma\|_{0,h} &\le ch\,\|f\|_{0,h}, \quad \textit{where} \quad \operatorname{div}\sigma = f, \\
\|H\|_{0,h} &\le ch\,\|\sigma\|_{0,h}, \quad \textit{where} \quad \operatorname{curl} H = \sigma, \\
\|u\|_{0,h} &\le ch\,\|H\|_{0,h}, \quad \textit{where} \quad \nabla u = H.
\end{aligned}$$

Proof. By transformation to the reference element (using standard, covariant, or the Piola transformation), one easily proves that

$$\begin{aligned}
\|f\|_{0,h}^2 &\simeq h^{-3}\Big\{\sum_T \big(\widehat{f_T}^{\,T}\big)^2 + \sum_F \big(\widehat{f_F}^{\,F}\big)^2 + \sum_E \big(\widehat{f_E}^{\,E}\big)^2 + \sum_V \big(f_V\big)^2\Big\}\\
\|\sigma\|_{0,h}^2 &\simeq h^{-1}\Big\{\sum_T \sum_{F\subset T} \big(\widehat{\sigma_T}^{\,F}\big)^2 + \sum_F \sum_{E\subset F} \big(\widehat{\sigma_F}^{\,E}\big)^2 + \sum_E \sum_{V\in E} \big(\widehat{\sigma_E}^{\,V}\big)^2\Big\}\\
\|H\|_{0,h}^2 &\simeq h^{1}\Big\{\sum_T \sum_{E\subset T} \big(\widehat{H_T}^{\,E}\big)^2 + \sum_F \sum_{E\subset F} \big(\widehat{H_F}^{\,E}\big)^2\Big\}\\
\|u\|_{0,h}^2 &\simeq h^{3}\Big\{\sum_T \sum_{V\in T} \big(\widehat{u_T}^{\,V}\big)^2\Big\}.
\end{aligned}$$

Define $\widehat{f}$ as the vector containing all degrees of freedom. The relation

$$\operatorname{div}\sigma = f$$

can be written as singular, but consistent matrix equation for the coefficient vectors

$$B_{\mathrm{div}}\widehat{\sigma} = \widehat{f}\,,$$

where the matrix B_{div} is defined according to (3.9). All matrix elements are either $+1$, -1, or 0. The matrix depends only on the topology of the mesh. Assuming a patch of shape regular elements, there is only a finite number of possible topologies, and thus there exists a common constant c such that

$$\|\widehat{\sigma}\,\|_{\mathbb{R}^n} \le c\,\|\widehat{f}\,\|_{\mathbb{R}^n}$$

Together with the norm equivalences there follows the statement. □

Similar arguments on matrices with entries $+1$, -1, and 0 in this context can be found in [13].

4. Equilibration in $H(\mathrm{curl})$

We consider the curl-curl equation for the vector potential: *Find* $u \in H(\mathrm{curl})$ *such that*

$$(\mu^{-1}\operatorname{curl} u, \operatorname{curl} v) = (j, v) \quad \text{for } v \in H(\mathrm{curl}).$$

The given current density j is supposed to be divergence free. Moreover, we assume that j is element-wise constant. Thus, j can be represented by means of Raviart–Thomas functions.

We are interested in a posteriori error estimates of the finite element discretization u_h with Nédélec elements of lowest order,

$$(\mu^{-1}\operatorname{curl} u_h, \operatorname{curl} v) = (j, v) \quad \text{for } v \in \mathcal{N}d.$$

The magnetic field H defined as

$$H := \mu^{-1} \operatorname{curl} u \tag{4.1}$$

satisfies Ampère's law

$$\operatorname{curl} H = j. \tag{4.2}$$

The magnetic field H_h obtained from the finite element discretization,

$$H_h := \mu^{-1} \operatorname{curl} u_h,$$

leads in general to a different current density

$$j_h := \operatorname{curl} H_h. \tag{4.3}$$

For piecewise linear vector potentials u_h, the magnetic flux H_h is piecewise constant, and the discrete curl, i.e. j_h, is a face-based RT distribution.

4.1. **An Equation of Prager–Synge Type.** The following result will be the basis of the error estimate. It is the analogue to Theorem 1.

Theorem 11. *Assume that $v \in H(\operatorname{curl})$ satisfies the boundary conditions and that $\tilde{H} \in H(\operatorname{curl})$ satisfies Ampère's law $\operatorname{curl} \tilde{H} = j$. Then*

$$\|\mu^{-1/2} \operatorname{curl}(u-v)\|_0^2 + \|\mu^{1/2}(H-\tilde{H})\|_0^2 = \|\mu^{-1/2}(\operatorname{curl} v - \mu\tilde{H})\|_0^2 . \tag{4.4}$$

Proof. Integration by parts yields the orthogonality relation

$$\begin{aligned}
&\int_\Omega \operatorname{curl}(u-v)(H-\tilde{H}) \\
&\qquad = \int_\Omega (u-v) \operatorname{curl}(H-\tilde{H}) + \int_{\partial\Omega} [(u-v)\times n]\cdot(H-\tilde{H}) \\
&\qquad = \int_\Omega (u-v)(j-j) = 0.
\end{aligned}$$

By applying the Binomial formula to $\mu^{-1/2} \operatorname{curl}(u-v) + \mu^{1/2}(\tilde{H}-H)$ and noting that $\mu H = \operatorname{curl} u$ we obtain (4.4). □

The lemma above will be applied to $v := u_h$. In order to achieve a good candidate for $\tilde{H}$ we have to solve $\operatorname{curl}(\tilde{H} - H_h) = j - j_h$. For this reason we are going to construct a correction H^Δ such that

$$j - j_h = \operatorname{curl} H^\Delta.$$

Again, we construct H_{ω_V} locally on the vertex patch ω_V such that we obtain a decomposition

$$H^\Delta = \sum H_{\omega_V}.$$

The construction will be independent of the material parameter μ, and μ will enter only at the final end when Theorem 11 will be applied.

4.2. **The Discrete Current.** The distribution j_h is evaluated by using partial integration and recalling that H_h is piecewise constant

$$\begin{aligned}\langle j_h, v\rangle &= \langle \operatorname{curl} H_h, v\rangle = (H_h, \operatorname{curl} v)\\ &= \sum_T \int_T \operatorname{curl} H_h \cdot v\, dx + \sum_F \int_F [H_h \times n]\cdot v\, ds\\ &= \sum_F ([H_h \times n], v)_F\,.\end{aligned}$$

The discrete current distributions are

$$j_{h,F} = [H_h \times n]. \tag{4.5}$$

Both currents, the prescribed current j as well as the discrete current j_h can be represented by distributional Raviart–Thomas elements of order 1. Both currents are divergence free.

We utilize the properties of the Galerkin orthogonality, namely

$$\left\langle j - j_h, \varphi^E \right\rangle = 0 \tag{4.6}$$

for each Nédélec basis functions φ^E associated with the generic edge E. Let V_1 and V_2 be its two vertices. Given an edge E of an element T, the basis function can be expressed on the simplex T in terms of the barycentric coordinates

$$\varphi^E = \lambda_1 \nabla\lambda_2 - \lambda_2 \nabla\lambda_1\,;$$

see [14, (5.47)]. We recall that j as well as $\nabla\lambda_i$ are constant on the element and evaluate the contribution of j on an element T sharing the edge E:

$$\begin{aligned}\int_T j\cdot\varphi^E &= \int_T j\cdot(\lambda_1\nabla\lambda_2 - \lambda_2\nabla\lambda_1)\\ &= (j\cdot\nabla\lambda_2)\int_T \lambda_1 - (j\cdot\nabla\lambda_1)\int_T \lambda_2\\ &= \frac{|T|}{4}\left\{j\cdot\nabla\lambda_2 - j\cdot\nabla\lambda_1\right\}.\end{aligned}$$

Now, observe that $\nabla\lambda_i$ is proportional to the normal vector on the face F_i which lies opposite to vertex V_i, and the factor is the inverse of the height of the element over the face F_i:

$$\nabla\lambda_i = -h_i^{-1} n_i = -\frac{|F_i|}{3|T|} n_i.$$

Thus, the element contributions evaluate to

$$\begin{aligned}\int_T j\cdot\varphi^E &= \frac{1}{12}\left\{|F_1|\, j\cdot n_1 - |F_2|\, j\cdot n_2\right\}\\ &= \frac{1}{12}\Big\{\int_{F_1} j\cdot n - \int_{F_2} j\cdot n\Big\} = \frac{1}{12}\left\{\widehat{j_T}^{\,F_1} - \widehat{j_T}^{\,F_2}\right\}. \quad (4.7)\end{aligned}$$

Note that the fluxes through element faces are the degrees of freedom of the Raviart–Thomas elements.

Similarly, the contributions of j_h on a face F is determined

$$\begin{aligned}\int_F j_{h,F}\cdot\varphi^E &= \frac{1}{6}\Big\{\int_{E_1} j_h\cdot n - \int_{E_2} j_h\cdot n\Big\}\\ &= \frac{1}{6}\big\{\widehat{j_{h,F}}^{\,E_1} - \widehat{j_{h,F}}^{\,E_2}\big\}\end{aligned}$$

where V_1, V_2 are the end points of E, and E_1, E_2 are the edges of the face F which lie opposite to the vertices above. The normal vectors to the edges refer to the plane F and are vectors in F.

The integrals above are inserted in (4.6) to derive a relation between the original and the discrete current

$$\begin{aligned}&\frac{1}{12}\sum_{T:E\subset T}\Big\{\textstyle\int_{F_{T,1}} j\cdot n - \int_{F_{T,2}} j\cdot n\Big\}\\ &\qquad = \frac{1}{6}\sum_{F:E\subset F}\Big\{\textstyle\int_{E_{F,1}} j_h\cdot n - \int_{E_{F,2}} j_h\cdot n\Big\}\end{aligned} \quad (4.8)$$

or

$$\frac{1}{12}\sum_{T:E\subset T}\big\{\widehat{j_T}^{\,F_{T,1}} - \widehat{j_T}^{\,F_{T,2}}\big\} - \frac{1}{6}\sum_{F:E\subset F}\big\{\widehat{j_{h,F}}^{\,E_{F,1}} - \widehat{j_{h,F}}^{\,E_{F,1}}\big\} = 0. \quad (4.9)$$

4.3. **Equilibration in 2D.** The basic relation for the 2D model that corresponds to (4.9) can be established in the same way

$$\frac{1}{6}\sum_{T:E\subset T}\big\{\widehat{j_T}^{\,E_{T,1}} - \widehat{j_T}^{\,E_{T,2}}\big\} + \frac{1}{2}\big\{\widehat{j_{h,E}}^{\,V_1} - \widehat{j_{h,E}}^{\,V_2}\big\} = 0. \quad (4.10)$$

As above, V_1, V_2 are the end points of the edge E under consideration, and $E_{T,1}$, $E_{T,2}$ are the edges of the triangle T that lie opposite to them; see Figure 7. (The sign of the second term in (4.10) differs from that in (4.9) since V_1, V_2 refer directly to the points and not to objects opposite to them.)

We proceed with the 2D case and are going to decompose the residual current into local, divergence free currents, i.e.,

$$j - j_h = \sum_V j_{\omega_V}\,.$$

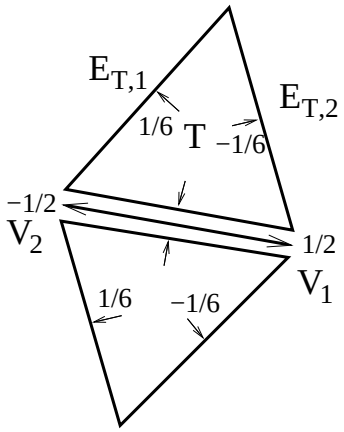

FIGURE 7. Factors in relation (4.10) referring to an edge and adjacent triangles. The edge terms refer to j and the vertex terms to j_h.

We consider a generic node V and the patch $\omega_V := \cup\{T,\ V \in \partial T\}$. Let T be a triangle in ω_V and E be an edge of the triangle sharing the vertex V. The edge of the triangle T opposite to V is denoted as $E_{T,O}$. It is located on the boundary of ω_V. The third edge is denoted as $E_{T,P}$. We define the local current j_{ω_V} on T by

$$\begin{aligned}
\widehat{j_{\omega_V,T}}^{E} &:= \frac{1}{2}\widehat{j_T}^{E} + \frac{1}{6}(\widehat{j_T}^{E_{T,O}} - \widehat{j_T}^{E_{T,P}})\,, \\
\widehat{j_{\omega_V,T}}^{E_P} &:= \frac{1}{2}\widehat{j_T}^{E_{T,P}} + \frac{1}{6}(\widehat{j_T}^{E_{T,O}} - \widehat{j_T}^{E})\,, \\
\widehat{j_{\omega_V,T}}^{E_O} &:= 0.
\end{aligned} \tag{4.11}$$

Obviously, the setting is symmetric with respect to the two edges that share the vertex V, but the representation with respect to a given edge E will be more useful in the sequel. Moreover, the flow is fixed such that the flow on the boundary of ω_V is zero.

Next, let E be an edge in the patch ω_V that connects V with a point V_O on $\partial\omega_V$. The vertex distributional parts are now fixed and evaluated from the fluxes on E via

$$\begin{aligned}
\widehat{j_{\omega_V,E}}^{V} &:= -\widehat{j_{h,E}}^{V}\,, \\
\widehat{j_{\omega_V,E}}^{V_O} &:= 0\,.
\end{aligned} \tag{4.12}$$

By definition, this current has also zero flow on $\partial\omega_V$.

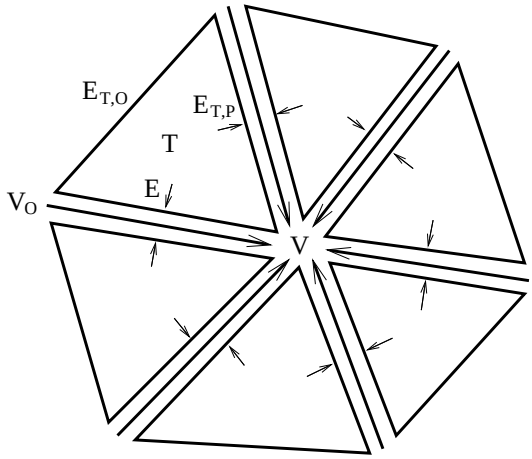

FIGURE 8. Some notation for the local current j_{ω_V}

Lemma 12. *If j_{ω_V} is defined by (4.11) and (4.12), then* $\operatorname{div} j_{\omega_V} = 0$ *and we have a decomposition*

$$j - j_h = \sum_V j_{\omega_V} . \tag{4.13}$$

Proof. Let T be a triangle with edge E whose endpoints are V_1 and V_2. When we sum over all patches, only the patches with centers V_1 and V_2 contribute to the sum of $\widehat{j_{\omega_V,T}}^{\,E}$. Recalling (4.11) we have

$$\begin{aligned} \sum_V \widehat{j_{\omega_V,T}}^{\,E} &= \widehat{j_{\omega_{V_1},T}}^{\,E} + \widehat{j_{\omega_{V_2},T}}^{\,E} \\ &= \frac{1}{2}\widehat{j_T}^{\,E} + \frac{1}{2}\widehat{j_T}^{\,E} = \widehat{j_T}^{\,E} \end{aligned}$$

since the terms with the factor 1/6 in (4.11) cancel in the sum. Moreover, only the patch with center V contributes to the sum of $\widehat{j_{\omega_V,E}}^{\,V}$, Hence,

$$\sum_{V'} \widehat{j_{\omega_{V'},E}}^{\,V} = \widehat{j_{\omega_V,E}}^{\,V} = -\widehat{j_{h,E}}^{\,V} .$$

The last two equations show that (4.13) holds.

We consider now the divergence of j_{ω_V} and do it recalling (3.9). By adding the terms in (4.11) it follows that

$$\begin{aligned}
\widehat{\operatorname{div} j_{\omega_V}}^{\,T} &= \sum_{E:E\subset T} \widehat{j_{\omega_V,T}}^{\,E} = \widehat{j_{\omega_V,T}}^{\,E} + \widehat{j_{\omega_V,T}}^{\,E_{T,P}} + \widehat{j_{\omega_V,T}}^{\,E_{T,O}} \\
&= \frac{1}{2}\widehat{j_T}^{\,E} + \frac{1}{6}(\widehat{j_T}^{\,E_{T,O}} - \widehat{j_T}^{\,E_{T,P}}) \\
&\quad + \frac{1}{2}\widehat{j_T}^{\,E_{T,P}} + \frac{1}{6}(\widehat{j_T}^{\,E_{T,O}} - \widehat{j_T}^{\,E}) + 0 \\
&= \frac{1}{3}\{\widehat{j_T}^{\,E} + \widehat{j_T}^{\,E_{T,O}} + \widehat{j_T}^{\,E_{T,P}}\} \\
&= \frac{1}{3}\int_{\partial T} j\cdot n = \frac{1}{3}\int_T \operatorname{div} j = 0. \qquad (4.14)
\end{aligned}$$

We obtain the edge terms from (4.11) and (4.12)

$$\begin{aligned}
\widehat{\operatorname{div} j_{\omega_V}}^{\,E} &= \widehat{j_{\omega_V,E}}^{\,V} + \widehat{j_{\omega_V,E}}^{\,V_{E,O}} - \sum_{T:E\subset T} \widehat{j_{\omega_V,T}}^{\,E} \\
&= -\widehat{j_{h,E}}^{\,V} + 0 - \sum_{T:E\subset T} \{\frac{1}{2}\widehat{j_T}^{\,E} + \frac{1}{6}\big(\widehat{j_T}^{\,E_{T,O}} - \widehat{j_E}^{\,E_{T,P}}\big)\}. \qquad (4.15)
\end{aligned}$$

Since the normal components of j are continuous, we have $\sum_{T:E\subset T}\frac{1}{2}\widehat{j_T}^{\,E} = 0$. From $\operatorname{div} j_h = 0$ it follows that $\widehat{j_{h,E}}^{\,V} + \widehat{j_{h,E}}^{\,V_O} = 0$, and we continue with

$$\widehat{\operatorname{div} j_{\omega_V}}^{\,E} = -\frac{1}{2}\big(\widehat{j_{h,E}}^{\,V} - \widehat{j_{h,E}}^{\,V_O}\big) - \sum_{T:E\subset T}\frac{1}{6}\big(\widehat{j_T}^{\,E_{T,O}} - \widehat{j_E}^{\,E_{T,P}}\big) = 0.$$

Here we applied the Galerkin equation (4.10) to $V_1 = V$ and to $V_2 = V_O$.

Finally, the vertex terms are given by the flow into the center of the patch. From the definition (4.12) we have

$$\widehat{\operatorname{div} j_{\omega_V}}^{\,V} = \sum_{E:V\in E}\widehat{j_{\omega_V,E}}^{\,V} = \sum_{E:V\in E}\widehat{-j_{h,E}}^{\,V} = -\widehat{\operatorname{div} j_h}^{\,V} = 0. \qquad (4.16)$$

This concludes the proof of $\operatorname{div} j_{\omega_V} = 0$. □

We note that (4.16) can be obtained from (4.14) and (4.15) by virtue of arguments in the spirit of Remark 7. Since the current vanishes on $\partial\omega_V$ and the divergence on the triangles and the slim rectangles is zero, the total flux into V must also be zero. (This argument is also helpful in the 3-dimensional case.)

Since j_{ω_V} is in $\mathcal{R}T_{-2}$ with vanishing boundary values, we can apply the second distributional de Rham sequence to find an H_{ω_V} in the

scalar non-continuous P^1 space $\mathcal{M}^1_{-1}$ with vanishing boundary values such that

$$\operatorname{curl} H_{\omega_V} = j_{\omega_V}.$$

Recalling (3.10) we see that H_{ω_V} is easily determined.

Remark 13. *Since the right-hand side of (4.15) vanishes, we conclude from (4.15) that the current j_h can be expressed in terms of j. Therefore, j_h, j_{ω_V}, and the a posteriori error bound can be determined before the computation of the finite element solution. Moreover, the current of the decomposition is computed very locally, i.e. $j_{\omega_V,T}$ depends only on j_T and V, and $j_{\omega_V,E}$ depends only on $j_{h,E}$ and V.*

4.4. **Equilibration in 3D.** We consider the construction in the 3-dimensional case very briefly. We construct the local current on the patch around a generic vertex V. Regard a tetrahedron T, a face F and an edge E such that $V \in E \subset F \subset T$. Let $F_{T,O}$ be the face opposite to V, let $F_{T,P}$ be the face containing V and opposite to E, and let $F_{T,Q}$ be the remaining face containing E. Similarly, let $E_{F,O}$ be the edge of the face opposite to V and $E_{F,P}$ the edge of F containing the vertex V. The face terms on a tetrahedron depend only on j in T; cf. (4.11). We set

$$\widehat{j_{\omega_V,T}}^{F} := \frac{1}{3}\widehat{j_T}^{F} + \frac{1}{12}\widehat{j_T}^{F_{T,O}} - \frac{1}{24}\Big\{\widehat{j_T}^{F_{T,P}} + \widehat{j_T}^{F_{T,Q}}\Big\}. \tag{4.17}$$

By symmetry, this defines also the fluxes through $F_{T,P}$ and $F_{T,Q}$. Moreover, the flux on the boundary of the patch is set to zero

$$\widehat{j_{\omega_V,T}}^{F_{T,O}} := 0.$$

Contrary to the 2D case, the fluxes through faces depend not only on fluxes in faces, but involve also element terms. We set

$$\begin{aligned}\widehat{j_{\omega_V,F}}^{E} \;:=\; & -\Big\{\frac{1}{2}\widehat{j_{h,F}}^{E} + \frac{1}{6}\widehat{j_{h,F}}^{E_{F,O}} - \frac{1}{6}\widehat{j_{h,F}}^{E_{F,P}}\Big\} \\ & + \sum_{T:F\subset T} \frac{1}{24}\Big\{\widehat{j_T}^{F_{T,O}} - \widehat{j_T}^{F_{T,P}}\Big\}.\end{aligned} \tag{4.18}$$

Again, fluxes through the outer face are set to zero, i.e. $\widehat{j_{\omega_V,F}}^{E_{F,O}} = 0$.

Lemma 14. *This is a local, divergence free decomposition of the residual, i.e.,*

$$j - j_h = \sum_V j_{\omega_V},$$

and

$$\operatorname{div} j_{\omega_V} = 0.$$

We abandon the proof that proceeds along the lines of the proof of Lemma 12.

The results of this section are summarized for the Maxwell equation in 3-space as follows.

Theorem 15. *For each node V there exists a broken Nédélec-function H_{ω_V} with support in ω_V such that*

$$\operatorname{curl} H_{\omega_V} \;=\; j_{\omega_V}$$

holds in distributional sense, where j_{ω_V} is defined by (4.17) and (4.18). Choose H_{ω_V} with (quasi-) minimal L_2-norm, and let $H^\Delta := \sum_V H_{\omega_V}$.

Then the postprocessed magnetic flux $\tilde{H} = \mu^{-1} \operatorname{curl} u_h + H^\Delta$ satisfies Ampère's law $\operatorname{curl} \tilde{H} = j$, and we have the a posteriori error estimate

$$c_0 \|\mu^{1/2} H^\Delta\| \;\le\; \|\mu^{-1/2} \operatorname{curl}(u - u_h)\| \;\le\; \|\mu^{1/2} H^\Delta\|. \tag{4.19}$$

Proof. The reliability follows from Lemma 14, the exactness of the second distributional de Rham sequence (3.17), and Theorem 11. The efficiency estimate follows from the stability of the right inverse, Lemma 10, and the efficiency of the residual error estimator analyzed in [6]. □

Acknowledgement. The authors are grateful to Professor Ulrich Langer for the stimulating atmosphere at the "Special Radon Semester on Computational Mechanics" that he organized in Linz in 2005. The first author thanks also Professor Sergei Repin for interesting discussions in addition to his lectures on a posteriori error estimates.

References

[1] Ainsworth, M. and Oden, T.J. (2000): A Posteriori Error Estimation in Finite Element Analysis. Wiley, Chichester.

[2] Arnold, D.N., Falk, R.S. and Winther, R. (2000): Multigrid in $H(div)$ and $H(curl)$. Numer. Math. 85, 197–217

[3] Arnold, D.N., Falk, R.S. and Winther, R. (2006): Differential complexes and stability of finite element methods. I. The de Rham complex. In "Proceedings of the IMA workshop on Compatible Spatial Discretizations for PDE" pp. 23–46

[4] Arnold, D.N., Falk, R.S. and Winther, R. (2006): Finite element exterior calculus, homological techniques, and applications. Acta Numerica (to appear)

[5] Bank, R.E. and Weiser, A. (1985): Some a posteriori error estimators for elliptic partial differential equations. Math. Comp. 44, 283–301

[6] Beck, R., Hiptmair, R., Hoppe, R., and Wohlmuth, B. (2000): Residual based a posteriori error estimators for eddy current computations. M^2AN, 34(1), 159–182

[7] Bossavit, A. (2005): Discretization of electromagnetic problems: The "General finite differences", In "Handbook of Numerical Analysis. Volume XIII (Ciarlet, P.G. ed.), pp. 105–197. Elsevier, Amsterdam

[8] Braess, D. (2001): Finite Elements: Theory, Fast Solvers and Applications in Solid Mechanics. Cambridge University Press.
[9] Brezzi, F. and Fortin, M. (1991): Mixed and Hybrid Finite Element Methods. Springer-Verlag, Berlin – Heidelberg – New York
[10] Demkowicz, L. (2006): Computing with *hp* Finite Elements. I. One- and Two-Dimensional Elliptic and Maxwell Problems. CRC Press, Taylor and Francis.
[11] Hiptmair, R. (2002): Finite elements in computational electromagnetism Acta Numerica 2002, 237–339
[12] Ladeveze, P. and Leguillon, D. (1983): Error estimate procedure in the finite element method and applications. SIAM J. Numer. Anal. 20, 485–509
[13] Luce, R. and Wohlmuth, B. (2004): A local a posteriori error estimator based on equilibrated fluxes. SIAM J. Numer. Anal. 42, 1394–1414
[14] Monk, P. (2003): Finite Element Methods for Maxwell's Equations. Clarendon Press, Oxford
[15] Nédélec, J.C. (1986): A new family of mixed finite elements in $\mathbb{R}^3$. Numer. Math. 50, 57–81.
[16] Neittaanmäki, P. and Repin, S. (2004): Reliable Methods for Computer Simulation. Error control and a posteriori estimates. Elsevier. Amsterdam
[17] Prager, W. and Synge, J.L. (1949): Approximations in elasticity based on the concept of function spaces. Quart. Appl. Math. 5, 241–269
[18] Schöberl, J. (2006): A posteriori error estimates for Maxwell equations. Math. Comp. (submitted),
[19] Vejchodský, T. (2004): Local a posteriori error estimator based on the hypercircle method. In " Proc. of the European Congress on Computational Methods in Applied Sciences and Engineering" (ECCOMAS 2004), Jyvaskylä, Finland.
[20] Verfürth, R. (1996): A Review of A Posteriori Error Esimation and Adaptive Mesh-Refinement Techniques. Wiley-Teubner, Chichester – New York – Stuttgart

URL: `http://www.hpfem.jku.at/people/joachim`
Current address: Faculty of Mathematics, Ruhr-University, D 44780 Bochum, Germany, – Center for Computational Engineering Science, RWTH Aachen University, D 52062 Aachen, Germany, – Dietrich.Braess@rub.de, – joachim.schoeberl@mathcces.rwth-aachen.de